Domain nucleation processes in mesoscopic $Ni_{80}Fe_{20}$ wire junctions

W. Y. Lee, C. C. Yao, A. Hirohata, Y. B. Xu, H. T. Leung, S. M. Gardiner, S. McPhail, B. C. Choi, D. G. Hasko, and J. A. C. Bland[a)]
Cavendish Laboratory, University of Cambridge, Cambridge, CB3 0HE, United Kingdom

(Received 3 September 1999; accepted for publication 6 December 1999)

The magnetization reversal process in permalloy ($Ni_{80}Fe_{20}$) wire junction structures has been investigated using magnetoresistance (MR) measurements and scanning Kerr microscopy. A combination of electron beam lithography and a lift-off process has been utilized to fabricate wires consisting of two 200 μm length regions with distinct widths w_1 and w_2 in the range 1–5 μm. Longitudinal MR measurements and magneto-optic Kerr effect hysteresis loops demonstrate that the magnetization reversal of the complete structure is predominantly determined by the wider region for fields applied parallel to the wire axis. Magnetic force microscopy and micromagnetic calculations show that several domain walls nucleate in the wider part and are trapped in the junction area. This implies that domain nucleation at the junction of the wire initiates magnetization reversal in the narrow half. As a consequence, the switching fields are found to be identical in both halves in this case. These results suggest the possibility of designing structures which can be used to ''launch'' reverse domains in narrow wires within a controlled field range. © *2000 American Institute of Physics.* [S0021-8979(00)01306-2]

I. INTRODUCTION

Advances in lithography and pattern transfer techniques have provided the opportunity of exploring novel magnetic phenomena in laterally controlled structures. In particular, the characteristics of magnetic stripes have been extensively investigated because of their importance in both magnetoresistance (MR) devices[1–16] and, more recently, magnetoelectronic devices.[17,18] There have been numerous efforts[1–16] to investigate the magnetization reversal and MR behavior in ferromagnetic wires so far. Very recent studies[9–13] have demonstrated that the switching field and magnetization reversal process depend strongly on the end shape as well as the width of ferromagnetic wires. The effect of the end shape is attributed to the formation of end domains or edge domains, even in submicron structures, which are crucial in the magnetization reversal process.[9–13] A switching anomaly[11] associated with end domains for which the switching field is dependent on the applied field amplitude was observed in submicron ferromagnetic elements, which cannot be explained by the Stoner–Wohlfarth coherent rotation model. The shape of a wire structure has a decisive influence on magnetic properties in the micron size range. For example, the magnetization reversal process and MR behavior are found to change significantly in micron-sized $Ni_{80}Fe_{20}$ modulated width,[15] ''elbow''-shaped and cross-shaped wire structures[16] due to the modified shape-dependent demagnetizing fields.

In this article, we present a novel shape effect in extended permalloy ($Ni_{80}Fe_{20}$) wire junctions, leading to a striking variation in the switching field and magnetization reversal. We demonstrate that it is possible to control the switching field by introducing a junction that facilitates magnetization reversal in the narrow part. This result contrasts with the behavior found for symmetrically modified ends which suppress the formation of end domains in rectangular elements and so increase the switching field. Our results suggest the possibility of designing structures which can be used to ''launch'' reverse domains in narrow wires within a controlled field range, and which can be used for studies of magnetization reversal dynamics. We discuss the geometrical effect of the junction on the magnetization reversal and switching field associated with domain configurations inferred from magnetic force microscopy (MFM) imaging and micromagnetic calculations.

II. EXPERIMENT

A permalloy film was deposited at room temperature at a rate of $\sim$2 Å/min with a pressure of 6×10^{-9} mbar and then annealed at 120 °C for 30 min to remove the uniaxial anisotropy induced during deposition. A combination of electron beam lithography and a lift-off process has been utilized to fabricate wire array structures from a continuous film of 30 Å Au/300 Å $Ni_{80}Fe_{20}$/GaAs(001). Each wire consists of a narrow part (variable width w_1) and a wide part (fixed width w_2): the widths of the wires change abruptly at the midpoint to create two 200 μm length regions with $w_1=1{,}2$ μm and $w_2=5$ μm. Figure 1 shows a scanning electron microscopy (SEM) photograph of the wire junction structures ($w_1=1$ μm, $w_2=5$ μm). The separation between the centers of the wires is 15 μm, so that the magnetostatic interaction between wires is negligible.[8] Two fixed width wires ($w_1=w_2=1{,}5$ μm) were also produced as reference samples. In addition, we fabricated bridge-wire structures as shown in the schematics of Fig. 7(a) for magneto-optic kerr effect (MOKE) and MFM measurements. The bridge wire is a

a)Author to whom correspondence should be addressed; electronic mail: jacbl@phy.cam.ac.uk

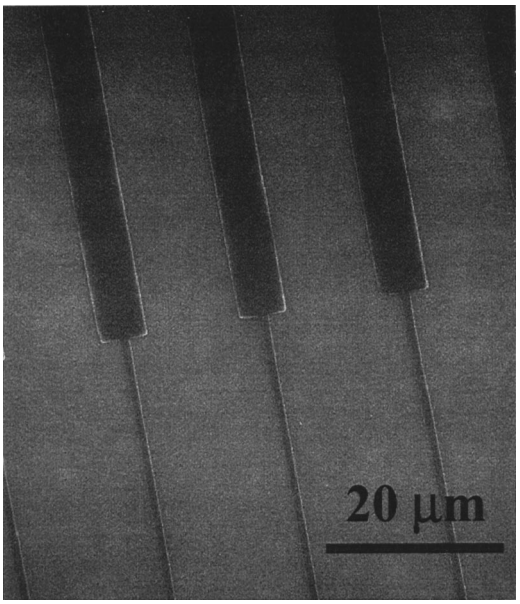

FIG. 1. A SEM photograph of the wire junction structures ($w_1=1\ \mu$m, $w_2=5\ \mu$m). The separation between the centers of the structure is 15 μm, so that the magnetostatic interaction is negligible.

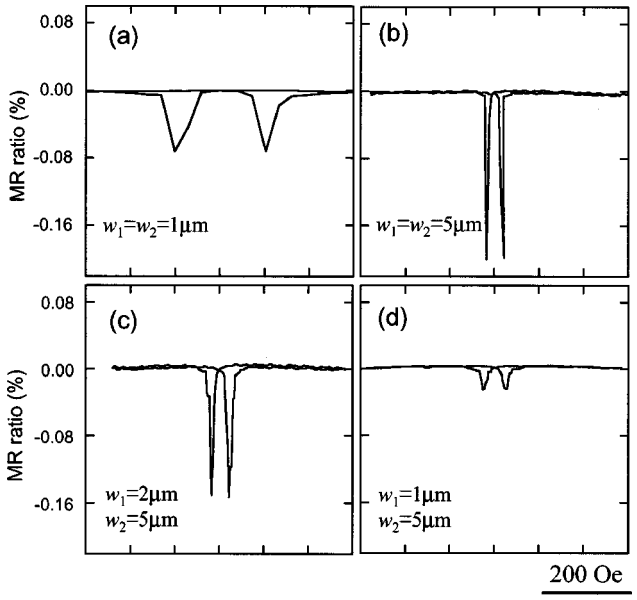

FIG. 2. Magnetoresistance (MR) response to magnetic fields along the wire axis for the fixed width wires and wire junction structures.

single wire ($l=205\ \mu$m and $w=10\ \mu$m) which has a narrow region of length $l=5\ \mu$m and width $w=0.5-10\ \mu$m in the center of the wire.

For MR measurements, standard optical lithography, metallization, and lift-off of 20 nm Cr/250 nm Au were utilized to fabricate electrical contacts to the arrays of 10 wires.[6,8] The voltage probes were separated by 160 μm. A dc current of 1 mA was passed along the wires and the resistance was measured using a four terminal method as the in-plane magnetic field was applied. The MR response to a magnetic field (H) applied parallel and perpendicular to the wire axis at room temperature is defined as $(R_H - R_{H=0})/R_{H=0}$, where R_H is the resistance at a given magnetic field. The hysteresis loops were obtained by scanning Kerr microscopy.[16,17] Two objective lenses (×20, Numerical Aperture: 0.55, ×50, NA: 0.85) were used to focus the probing laser beam (~3 μm, ~1 μm spot size, respectively) on the wires. Magnetic force microscopy (MFM, Digital Instruments) has been carried out so as to observe domain configurations of the wire junction structures and bridge wires.

III. RESULTS AND DISCUSSION

The MR response to magnetic fields applied along the wire axis for the fixed width wires (*a,b*) and wire junction structures (*c,d*) is presented in Fig. 2. The MR results for two fixed width wires, $w_1=w_2=1$ and 5 μm, in Figs. 2(a) and 2(b) are consistent with previous results[1,2,8] which show that the minimum resistance corresponds to the coercive field H_c. H_c is observed to increase with decreasing wire width due to buckling of the magnetization perpendicular to the wire, leading to the formation of domain walls perpendicular to the wire.[1,2,5,8] These walls prevent reverse domains from moving along the wire when the width is smaller than the buckling wavelength. Comparing the MR results of the fixed width wire ($w_1=w_2=5\ \mu$m) with those of the wire junction structures in Figs. 2(c) and 2(d), it is seen that the MR ratio decreases as the width w_1 is reduced to 1 μm, when $w_2=5\ \mu$m. While the change of the resistance ($\Delta\rho$) was in all cases $\sim 5.5\times 10^{-2}\ \Omega$, the zero field resistance ($R_{H=0}$) in the wire junction structures is bigger than that for the fixed width wire. This can be explained by numerically solving Poisson's equation utilizing the finite element method (FEM). Contributions to the zero field resistance by the narrow part (width w_1) for the wire junction structures ($w_1=2{,}1\ \mu$m and $w_2=5\ \mu$m), were calculated as 71.4% and 83.2% of the overall resistance, respectively. An interesting feature is that, regardless of width w_1, the coercive fields are approximately 20–24 Oe. In particular, the coercivity of the wire junction structures ($w_1=1\ \mu$m, $w_2=5\ \mu$m) in Fig. 2(d) is much smaller than the value of 102 Oe seen in the fixed width wire ($w_1=w_2=1\ \mu$m) in Fig. 2(a). Further details of the switching field will be discussed later.

Figure 3 shows at low field ($H<M_s$) the MR behavior in response to fields applied perpendicular to the wire axis for the fixed width (*a,b*) and wire junction structures (*c,d*). For the fixed width wires ($w_1=w_2=1{,}5\ \mu$m), the MR behavior is very similar to that found in earlier work.[8] Characteristic bell shaped MR curves are observed and the anisotropic MR is mainly attributed to spin rotation dominating the magnetization reversal process rather than domains forming across the width of the wire. The onset of a linear region associated with the Lorentz MR corresponds to magnetic saturation and depends upon the expected shape anisotropy. For the wire junction structures in Figs. 3(c) and 3(d) the narrow part ($w_1=1{,}2\ \mu$m) dominates the reversal process and transverse AMR. Two onset points for the two linear regions associated with each value of the shape anisotropy are noticeable [see Fig. 3(d): **A** indicates the half with $w_2=5\ \mu$m and **B** the half with $w_1=1\ \mu$m].

In order to explain the magnetization reversal behavior determined by longitudinal MR measurements in the wire

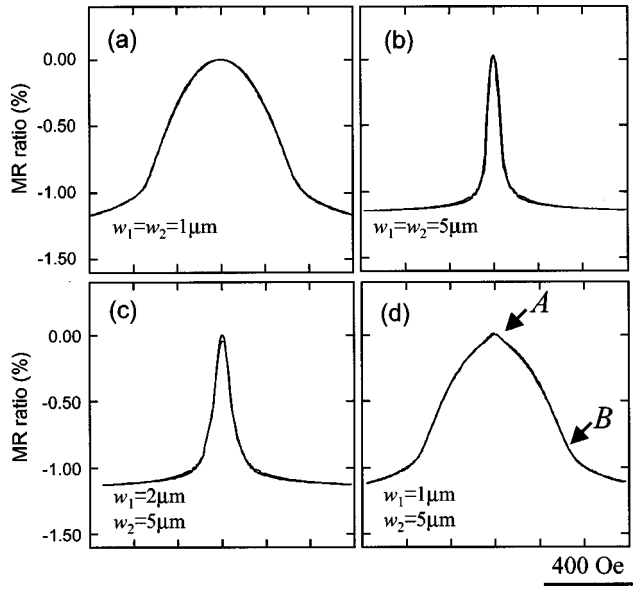

FIG. 3. Magnetoresistance (MR) response to magnetic fields along the hard axis for the fixed width wires and wire junction structures.

junction structures ($w_1=1$, $w_2=5\ \mu$m), scanning Kerr microscopy has been used to measure microscopic MOKE hysteresis loops. These were measured in eight different positions of the wire when magnetic fields were applied parallel to the wire axis, as shown in Fig. 4. In both halves ($w_1=1$ and $w_2=5\ \mu$m), coercive fields were determined as 22–23 Oe, which is in very good agreement with the MR results except at the ends and junction of the wire. Surprisingly, the coercive fields (*a,b,c* in Fig. 4) are quite different from the value of 102 Oe determined by MR measurements for the fixed width wires ($w_1=w_2=1\ \mu$m). Microscopic loops for the wide part ($w_2=5\ \mu$m) clearly show that the switching field depends on the inhomogeneous demagnetizing field (H_d) in the wire. In particular, a double-jump switching is observed in the junction of the wire: $H_{c1}=12$ and $H_{c2}=22$ Oe, as in Fig. 4(d). This proves the expected spatial variation in the demagnetizing field in the wire due to the free poles, which appear on its end and junction. This behavior can be understood in terms of two different effective shape anisotropies in the wire junction structure. On traveling across the wire from the wide part during magnetization reversal, domain walls are trapped in the junction, and cannot move further until a field of $H_{c2}=22$ Oe is reached. The double-jump switching disappears as the probing beam spot moves away from the junction by 5 and 10 μm as shown in Figs. 4(e) and 4(f), respectively. From the similar values of the coercive field in the wide and narrow parts we infer that the nucleation field (H_n) is greater than the wall motion field (H_w) in the narrow part. On the other hand, the coercive field is smaller at the end of the wide wire than in the center. Since reversal is initiated at the end by nucleation, we conclude that H_n is less than H_w in the wide part. Figure 5 shows that switching fields of the narrow part ($w_1=1\ \mu$m) are in the range 22–26 Oe, confirming that the magnetization reversal of the complete structure is determined by the wider region ($w_2=5\ \mu$m). Similar results were also obtained for the wire junction structure ($w_1=2\ \mu$m, $w_2=5\ \mu$m), where the switching fields were almost identical ($\sim$26 Oe) in both halves of the wire.

Figure 6 shows (a) a MFM image obtained at the junction area in the remanent state and (b) the calculated magnetization configurations for the wire junction structure ($w_1=1\ \mu$m, $w_2=5\ \mu$m). It was found that a few edge domains appear at the junction and the narrow end (not shown here), but a nearly single domain structure exists through the length as seen in Fig. 6(a). This is in good qualitative agreement with the remanent magnetization pattern obtained by micromagnetic simulations based on the Labonte algorithm[19] as shown in Fig. 6(b). MFM and micromagnetic calculations show that several domain walls are trapped in the junction

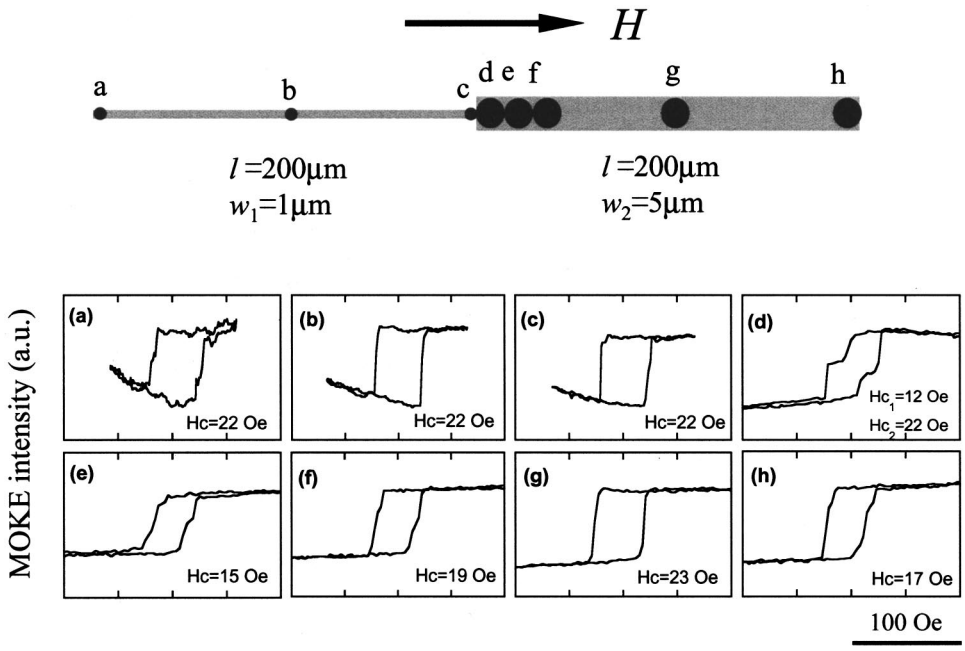

FIG. 4. MOKE hysteresis loops for a wire junction structure ($w_1=1\ \mu$m, $w_2=5\ \mu$m), measured in eight different positions by scanning Kerr microscope with 20× and 50× objective lenses. The dots on the wire denote approximate laser beam spot size.

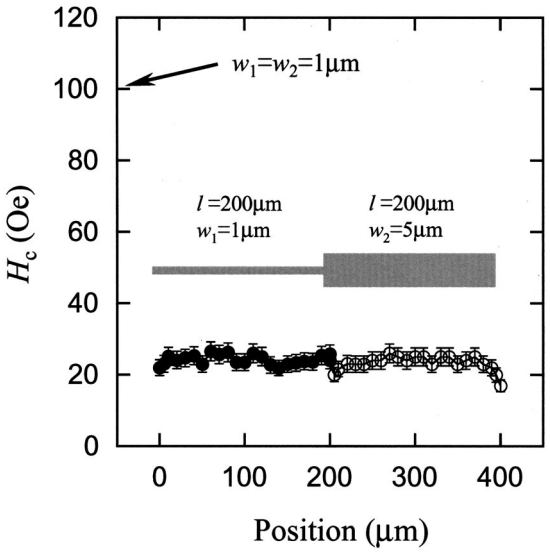

FIG. 5. Coercivity as a function of position for the wire junction structure ($w_1=1$ μm, $w_2=5$ μm), measured every 10 μm along the wire length. The arrow indicates H_c in the fixed width wire ($w_1=w_2=1$ μm).

area as observed. A detailed discussion of the results of micromagnetic calculations on the wire junction structures will be presented separately.[20]

Our results show that the junction in the wire junction structure facilitates magnetization reversal in the narrow part, in contrast to symmetrically modified ends such as pointed[9,10,12] and rounded[11,12] ends which suppress the formation of end domains in rectangular elements and increase the switching field. By accommodating multidomains in the vicinity of the flat end of the narrow wire, where it is harder to form reversed domains due to the higher magnetostatic energy in the corners, the junction offers a site for reversed domain wall nucleation in the narrow wire. In this way, the initiation of magnetization reversal occurs, and hence switching responds to a much smaller applied field than for a fixed width structure. This implies that the switching mechanism is dominated by domain wall nucleation rather than domain wall propagation in the permalloy wires and that the junction is crucial in initiating reversal. On the other hand, distinct reversal behavior has been observed in cross- and elbow-wire structures,[16] where domain-wall nucleation is facilitated or suppressed by the junction according to the wire width. For instance in cross and elbow structures, for $w<10$ μm the formation of reverse domains is suppressed due to the presence of a diagonal 180° wall at the junction induced by the perpendicular arms in the elbow and cross wires, giving rise to an increase in the switching field.[16]

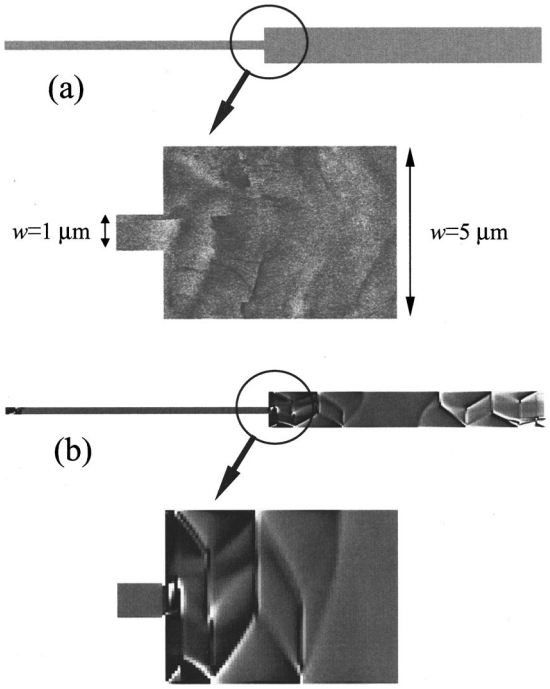

FIG. 6. (a) MFM image obtained at the junction area in the remanent state and (b) the remanent magnetization configurations of the junction obtained by micromagnetic simulations for the wire junction structure ($w_1=1$ μm, $w_2=5$ μm).

To better understand the magnetization reversal mechanism in the permalloy wires, we also fabricated bridge wires as shown in the schematics of Fig. 7(a) for MOKE and MFM measurements. The bridge wire is a single wire ($l=205$ and $w=10$ μm) which has a narrow region with a length $l=5$ μm and a width $w=0.5$–10 μm introduced in the center of the wire. MFM images indicate that narrow regions with $w\geqslant 5$ μm accommodate domain walls, whereas narrow regions with $w\leqslant 2$ μm show a single domain state [see Fig. 7(b): $w=1$ μm, (c): 0.5 μm]. MFM images also show multidomains appearing in the wide wires. The dots on the schematics in Fig. 7(a) denote the fixed positions **A** (50 μm away from the end of a wide wire) and **B** (center of the narrow wire) of the laser beam spots whose size were controlled according to the wire width. Figure 7(d) presents the variation in the coercive field (H_c) against the wire width of the narrow region. It is clearly seen that H_c does not vary with decreasing wire width but is identical ($H_c\approx 10$ Oe) in both regions. These results support the view that the switching mechanism is dominated by domain wall nucleation rather than domain wall propagation in the permalloy wires. The threshold field required for nucleation in the wire junction structure is much smaller than that of a single wire, while the field for domain wall motion is identical to that of the single wire, and is independent of the variable wire width in the micron range. In contrast to these results, we found that V necks introduced in the center of the wire increase the switching field in wide wires, which is similar to the effect of pointed ends.[21]

IV. CONCLUSION

The magnetization reversal process in permalloy ($Ni_{80}Fe_{20}$) wire structures has been investigated using magnetoresistance (MR) measurements and scanning Kerr microscopy. We find that the magnetization reversal of the wire junction structure is predominantly determined by the wider region in the structure for fields applied parallel to the wire axis. Domain nucleation at the junction of the wire initiates magnetization reversal in the narrow half so that the switching fields are identical in both halves. These results illustrate

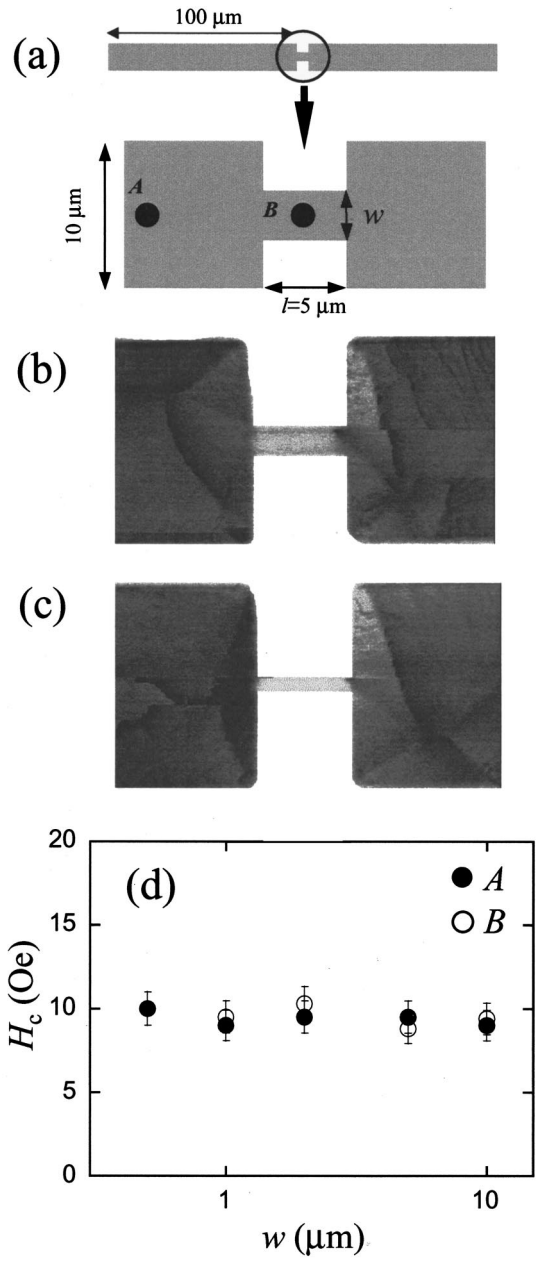

FIG. 7. (a) Schematics of the bridge structures, which have a narrow region with a length $l=5$ μm and a width $w=0.5-10$ μm introduced in the center of the wire. The dots on the schematics denote the fixed positions **A** (50 μm away from the end of a wide wire) and **B** (center of the narrow wire) of the laser beam spots. MFM images of the bridge structure with $w=1$ μm and $w=0.5$ μm are shown in (b) and (c) and the variation in the coercive field (H_c) against the wire width of the narrow region is shown in (d).

the possibility of lowering the switching field in narrow wires by introducing wider regions that nucleate reverse domains, in contrast to symmetrically modified ends which suppress the formation of end domains in rectangular elements. Our results suggest the possibility of designing structures which can be used to launch reverse domains in narrow wires within a controlled field range for applications such as magnetic sensor and spin electronic devices or for fundamental experiments in magnetization reversal dynamics.

ACKNOWLEDGMENTS

This work was supported by the EPSRC (U.K.) and also by the EU programs (''MASSDOTS'' and ''SUB-MAGDEV.'') W. Y. Lee wishes to thank the British Council Korea for the financial support.

[1] J. H. J. Fluitman, Thin Solid Films **16**, 269 (1973).
[2] M. H. Kryder, K. Y. Ahn, N. J. Mazzeo, S. Schwarzi, and S. M. Kane, IEEE Trans. Magn. **16**, 99 (1980).
[3] S. K. Decker, J. Dittmar, and C. Tsang, IEEE Trans. Magn. **17**, 2662 (1981); C. Tsang and S. K. Decker, J. Appl. Phys. **52**, 2465 (1981); C. Tsang and S. K. Decker, J. Appl. Phys. **53**, 2602 (1982).
[4] E. J. Ozimek and D. I. Paul, J. Appl. Phys. **55**, 2232 (1984).
[5] J. F. Smyth, S. Schultz, D. R. Fredkin, D. P. Kern, S. A. Rishton, M. Cali, and T. R. Koehler, J. Appl. Phys. **69**, 5262 (1991).
[6] C. Shearwood, S. J. Blundell, M. J. Baird, J. A. C. Bland, M. Gester, H. Ahmed, and H. P. Hughes, J. Appl. Phys. **75**, 5249 (1994); S. J. Blundell, C. Shearwood, M. Gester, M. J. Baird, J. A. C. Bland, and H. Ahmed, J. Magn. Magn. Mater. **135**, L17 (1994).
[7] K. Hong and N. Giordano, Phys. Rev. B **51**, 9855 (1995); J. Magn. Magn. Mater. **151**, 396 (1995); J. Phys.: Condens. Matter **10**, L401 (1995).
[8] A. O. Adeyeye, J. A. C. Bland, C. Daboo, D. G. Hasko, and H. Ahmed, J. Appl. Phys. **79**, 6120 (1996); A. O. Adeyeye, G. Lauhoff, J. A. C. Bland, C. Daboo, D. G. Hasko, and H. Ahmed, Appl. Phys. Lett. **70**, 1046 (1997); A. O. Adeyeye, J. A. C. Bland, C. Daboo, D. G. Hasko, and H. Ahmed, J. Appl. Phys. **82**, 469 (1997).
[9] K. J. Kirk, J. N. Chapman, and C. D. W. Wilkinson, Appl. Phys. Lett. **71**, 539 (1997); M. Rührig, B. Khamsehpour, K. J. Kirk, J. N. Chapman, P. Aitchison, S. McVite, and C. D. W. Wilkinson, IEEE Trans. Magn. **32**, 4452 (1996).
[10] T. Schrefl, J. Fidler, K. J. Kirk, and J. N. Chapman, J. Magn. Magn. Mater. **175**, 193 (1997).
[11] J. Shi, T. Zhu, M. Durlam, E. Chen, and S. Tehrani, IEEE Trans. Magn. **34**, 997 (1998); J. Shi, S. Tehrani, T. Zhu, Y. F. Zheng, and J. G. Zhu, Appl. Phys. Lett. **74**, 2525 (1999).
[12] J. McCord, A. Hurbert, G. Schröpfer, and U. Loreit, IEEE Trans. Magn. **32**, 4806 (1996).
[13] J. Gadbois, J. G. Zhu, W. Vavra, and A. Hurst, IEEE Trans. Magn. **34**, 1066 (1998).
[14] R. D. Gomez, T. V. Luu, A. O. Pak, K. J. Kirk, and J. N. Chapman, J. Appl. Phys. **85**, 2525 (1999).
[15] C. C. Yao, D. G. Hasko, Y. B. Xu, W. Y. Lee, and J. A. C. Bland, J. Appl. Phys. **85**, 1689 (1999).
[16] W. Y. Lee, Y. B. Xu, C. A. F. Vaz, A. Hirohata, H. T. Leung, C. C. Yao, B. C. Choi, J. A. C. Bland, F. Rousseaux, E. Cambril, and H. Launois, IEEE Trans. Magn. **35**, 3883 (1999).
[17] W. Y. Lee, S. Gardelis, B. C. Choi, Y. B. Xu, C. G. Smith, C. H. W. Barnes, D. A. Ritchie, E. H. Linfield, and J. A. C. Bland, J. Appl. Phys. **85**, 6682 (1999).
[18] F. G. Monzon, D. S. Patterson, and M. L. Roukes, J. Magn. Magn. Mater. **195**, 19 (1999).
[19] A. E. Labonte, J. Appl. Phys. **40**, 2450 (1969).
[20] H. T. Leung, A. Hirohata, W. Y. Lee, and J. A. C. Bland (unpublished).
[21] A. Hirohata, Y. B. Xu, C. C. Yao, W. Y. Lee, H. T. Leung, and J. A. C. Bland, J. Appl. Phys. (in press).